

MANJUSHRI: A Tool for Equivalence Checking of Quantum Circuits

Xuan Du Trinh¹[0009-0009-5610-462X], Meghana Sistla²[0000-0002-4215-0651], Nengkun Yu¹[0000-0003-1188-3032], and Thomas Reps³[0000-0002-5676-9949]

¹ Stony Brook University, Stony Brook, NY, USA

² University of Texas at Austin, Austin, TX, USA

³ University of Wisconsin–Madison, Madison, WI, USA

Abstract. Verifying whether two quantum circuits are equivalent is a central challenge in the compilation and optimization of quantum programs. We introduce MANJUSHRI,⁴ a new automated framework for scalable quantum-circuit equivalence checking. MANJUSHRI uses local projections as discriminative circuit fingerprints, implemented with weighted binary decision diagrams (WBDDs), yielding a compact and efficient symbolic representation of quantum behavior.

We present an extensive experimental evaluation that, for random 1D Clifford+ T circuits, explores the trade-off between MANJUSHRI and ECMC, a tool for equivalence checking based on a much different approach. MANJUSHRI is much faster up to depth 30 (with the crossover point varying from 39–49, depending on the number of qubits and whether the input circuits are equivalent or inequivalent): when inputs are equivalent, MANJUSHRI is about 10 \times faster (or more); when inputs are inequivalent, MANJUSHRI is about 8 \times faster (or more). For both kinds of equivalence-checking outcomes, ECMC’s success rate out to depth 50 is impressive on 32- and 64-qubit circuits: on such circuits, ECMC is almost uniformly successful. However, ECMC struggled on 128-qubit circuits for some depths. MANJUSHRI is almost uniformly successful out to about depth 38, before tailing off to about 75% at depth 50 (falling to 0% at depth 48 for 128-qubit circuits that are equivalent).

These results establish that MANJUSHRI is a practical and scalable solution for large-scale quantum-circuit verification, and would be the preferred choice unless clients need to check equivalence of circuits of depth > 38 .

Keywords: Quantum Circuits · Equivalence Checking · WBDDs.

1 Introduction

Program equivalence is a central concept in computer science, with broad applications in software engineering, compiler validation, optimization, and program

⁴ Manjushri, the Bodhisattva of Wisdom and the Blade, symbolizes sharp, analytical, and transcendent insight that severs false perceptions, attachments, and the mental barriers that cause emotional instability, while discerning even the subtlest differences.

analysis [6,5,11]. Techniques for reasoning about program behavior have been extended from deterministic programs to probabilistic and approximate settings, addressing uncertainty and noise in practical systems [2,4].

With the rise of quantum programming languages, the formal verification of quantum programs has received increasing attention [23,22,12,20]. In particular, a growing body of work focuses on reasoning about the equivalence of quantum programs and circuits [3,16,9,21,24].

Beyond logic-based approaches, computational methods for quantum-circuit equivalence checking have attracted substantial attention. Direct classical simulation of quantum circuits is generally infeasible because the quantum state space grows exponentially with the number of qubits. Formally, equivalence checking requires proving that the quantum channels induced by two circuits are identical for all possible input states. This task is particularly challenging because, although the underlying Hilbert space is finite-dimensional, its dimension is exponential in the number of qubits and the set of input states has infinite cardinality. Together, these factors make naive state-space enumeration or exhaustive testing fundamentally intractable. Existing methods provide strong theoretical guarantees for exact verification, but they neither scale to large circuits nor support efficient approximate reasoning. These limitations motivate the development of automated and scalable verification tools.

Recent work has begun exploring scalable methods for quantum circuit equivalence checking, including approaches based on weighted model counting (WMC) [10] and collections of local projections as constraints [24]. The WMC-based approach encodes the behavior of quantum circuits into weighted Boolean formulas, reducing equivalence checking to a sequence of weighted model-counting problems. This method, implemented in tools such as ECMC [10], supports universal gate sets, including non-Clifford gates like Toffoli, and can exploit parallelism for large-scale verification.

Projection-Based Equivalence Checking (PBEC) [24], on the other hand, aims to reduce verification complexity by exploiting the structure of shallow circuits. A major difficulty in understanding and verifying quantum circuits arises from multipartite entanglement, which correlates many qubits in ways that are difficult to analyze globally. The intuition behind PBEC is that the depth of a quantum circuit not only represents its running time but also influences the rate at which multipartite entanglement is generated. In shallow circuits, entanglement spreads only partially, so the global output state can often be well-approximated by its marginal distributions over small subsets of qubits. This observation suggests that equivalence checking of shallow circuits may be achievable by reasoning over these low-order marginals rather than the full infinite state space of exponential dimension.

Despite these promising directions, current methods still struggle when scaling to circuits with hundreds of qubits or significant depth. WMC-based methods face combinatorial explosion, and PBEC become less effective as entanglement spreads across larger subsystems. As a result, efficiently handling large, deep circuits remains an open challenge, highlighting a critical gap in practical

techniques for verifying quantum-circuit equivalence for near-term and future quantum computing devices.

In this paper, we present MANJUSHRI, an automated framework for scalable equivalence checking of quantum circuits via PBEC. MANJUSHRI uses weighted binary decision diagrams (WBDDs) to represent local projections, resulting in a compact and efficient symbolic representation of a quantum circuit’s behavior.

The experiments with MANJUSHRI reported in Section 3 complement the experiments in the original paper on PBEC [24]. In that paper, the benchmarks are 1D random circuits, where every 2-qubit gate is generated from a Haar distribution (created for a specified number of qubits n and a specified depth d). For checking equivalence,⁵ circuit sizes were quite limited: $12 \leq n \leq 100$ with depth $d = 3$. In the present paper, the benchmarks are random 1D Clifford+ T circuits⁶ and much larger: $n \in \{32, 64, 128\}$ and $1 \leq d \leq 50$. Moreover, Section 3 gives a detailed comparison of the relative performance of MANJUSHRI and the ECMC tool (which performs equivalence checking via model counting).

2 Background and Related Work

Qubits. A *qubit* is the basic unit of quantum information. In the computational basis $\{|0\rangle, |1\rangle\}$, a qubit state is $|\psi\rangle = \alpha|0\rangle + \beta|1\rangle$, where $\alpha, \beta \in \mathbb{C}$ and $|\alpha|^2 + |\beta|^2 = 1$. Measurement yields outcomes $|0\rangle$ and $|1\rangle$ with probabilities $|\alpha|^2$ and $|\beta|^2$, respectively.

Quantum States. A pure quantum state is a unit vector $|\psi\rangle$ in a Hilbert space that encodes the probabilistic behavior of a system. Quantum states may be expressed as superpositions of basis states.

Tensor Product and Multi-Qubit Systems. For an n -qubit system, the joint state space is constructed as the tensor (Kronecker) product of n two-dimensional qubit spaces, yielding a Hilbert space of dimension 2^n —i.e., the dimension grows exponentially with the number of qubits n . This exponential growth in dimensionality enables the representation of complex multi-qubit states, including entangled states, and forms the mathematical foundation for modeling multi-qubit quantum gates.

Unitary Operations. Quantum evolution is described by unitary operators U satisfying $U^\dagger U = UU^\dagger = I$. This condition ensures reversibility and preserves state norms. Unitary operators acting on one or two qubits are called *quantum gates*.

The tensor (Kronecker) product combines operators that act on individual subsystems into a single operator on the composite system.

⁵ What we call “equivalence” in this paper was called “strong equivalence” in [24].

⁶ Our experiments check pairs of equivalent circuits (checking a given circuit C and $\text{Optimize}(C)$) and pairs of inequivalent circuits (checking C and $\text{Mutate}(\text{Optimize}(C))$). In both kinds of experiments, MANJUSHRI must handle more than Clifford+ T circuits because even if C is a Clifford+ T circuit, with the optimizer we are using, PyXZ [8], the circuit produced by $\text{Optimize}(C)$ can have R_z and CZ gates in it.

Quantum Circuits. Quantum circuits define unitary transformations over an n -qubit Hilbert space through a sequence of gate layers. Each layer consists of gates acting on disjoint subsets of qubits and can therefore be executed in parallel. For clarity, we focus on circuits composed of one- and two-qubit gates; all results extend directly to gates acting on at most a fixed constant number m of qubits.

Let $U_i^{(k)}$ denote the gate applied to qubit(s) indexed by i in layer k . The unitary operator corresponding to layer k is defined as $U^{(k)} = \bigotimes_i U_i^{(k)}$. A circuit of depth L is interpreted as the sequential composition of these layer operators, yielding the overall transformation

$$|\psi_{\text{out}}\rangle = U^{(L)} U^{(L-1)} \cdots U^{(1)} |\psi_{\text{in}}\rangle. \quad (1)$$

This formulation captures the operational semantics of a quantum circuit as a product of layer-wise unitary transformations. A unitary U induces a quantum operation on density matrices by conjugation. For a pure state $\rho = |\psi\rangle\langle\psi|$, we have $\mathcal{U}(\rho) := U\rho U^\dagger = U|\psi\rangle\langle\psi|U^\dagger$, where we define $\mathcal{U} := \lambda x. UxU^\dagger$. This coincides with the standard evolution of pure states.

Circuit Equivalence. Quantum states that differ by a global phase factor $e^{i\theta}$ are physically indistinguishable. This property motivates the notion of equivalence.

Definition 1 (Circuit equivalence). Two circuits $C_0 = \prod_{k=1}^L \bigotimes_i U_i^{(k)}$, and $C_1 = \prod_{k=1}^T \bigotimes_j V_j^{(k)}$ are equivalent if, for every input state n -qubit $|\psi\rangle$, their output states are equal up to a global phase.

Related Work

Scalable Equivalence Checking via Local Projections. Yu et al. [24] focused on shallow (constant-depth) quantum circuits and introduced Projection-Based Equivalence Checking (PBEC), which constructs a set of local-projection constraints that uniquely characterize a circuit’s output state, enabling equivalence checking without full state simulation. For circuits of fixed depth, the PBEC algorithm for checking equivalence runs in time and space linear in the number of qubits, exploiting the fact that a small set of local constraints suffices to capture the output state. Beyond equivalence checking, this representation also supports sound and complete assertion checking for properties expressed as conjunctions of local projections. Experimentally, equivalence checking between 100-qubit circuits of depth 3 took a few seconds to tens of seconds, and computing the constraint description for a 100-qubit circuit of depth 6 required under 20 seconds on large-memory multi-core hardware, demonstrating the practical scalability of the approach.

Equivalence Checking of Quantum Circuits via Model Counting. Mei et al. [10] reduces the n -qubit circuit equivalence problem, $\lambda x. UxU^\dagger = \lambda x. VxV^\dagger$, to $2n$ matrix-equality conditions, $\lambda x. UxU^\dagger P_i = \lambda x. VxV^\dagger P_i$, where each P_i is

a single-qubit Pauli matrix X or Z and each condition involves two $2^n \times 2^n$ matrices. The ECMC tool extends Pauli coefficient updates from Clifford circuits to Clifford+T+Toffoli circuits when appending a new gate layer and encodes these coefficients as weighted model counts, summing the weights of all satisfying assignments of a Boolean formula.

Quasimodo. Quasimodo⁷ [13] is an open-source Python library for symbolic simulation of quantum circuits, which supports different kinds of decision diagrams as the underlying data structure for representing gates, unitary matrices, etc.—in particular, CFLOBDDs [15], WCFLLOBDDs [14], BDDs (specifically CUDD [1]), and Weighted BDDs (WBDDs, specifically MQTDD [25]). MANJUSHRI uses Quasimodo to implement the PBEC algorithm [24]. For the experiments described in Section 3, MANJUSHRI was instantiated with WBDDs as the back-end representation; we found that for PBEC, the other kinds of decision diagrams supported by Quasimodo were not competitive.

3 Experiments

3.1 Experimental Setup

(1) *Compared tools and methods.* We benchmarked ECMC [10] against MANJUSHRI,⁸ our implementation of PBEC [24]. MANJUSHRI uses the MQTDD⁹ data structure [25] (essentially an implementation of WBDDs), for representing and manipulating circuit semantics. All input circuits are provided in QASM format. While ECMC operates directly on the QASM inputs, MANJUSHRI first converts each QASM circuit into an MQTDD-based internal representation. Accordingly, unless stated otherwise, the reported runtime for MANJUSHRI is defined as

$$T_{\text{MANJUSHRI}} = T_{\text{convert}} + T_{\text{check}},$$

where T_{convert} denotes QASM-to-MQTDD conversion time and T_{check} denotes equivalence-checking time on the converted representation. The reported runtime for ECMC corresponds to its equivalence-checking procedure on the original QASM inputs. All runs enforce a per-instance timeout of 100 seconds. The equivalence tolerance is set to 1×10^{-15} for both tools: MANJUSHRI uses this value as its numerical comparison tolerance between density matrices (see [24]), and ECMC uses it as the floating-point-error (FPE) threshold in the backend solver configuration.

The experiments were run on a server equipped with $2 \times$ Intel® Xeon® Gold 6338 CPUs (128 threads total) and 1.0 TiB of RAM, running Ubuntu 20.04.6 LTS.

⁷ <https://github.com/trishullab/Quasimodo>

⁸ MANJUSHRI is available as the “equivalence” branch of Quasimodo (<https://github.com/trishullab/Quasimodo/tree/equivalence>).

⁹ We made minor modifications to MQTDD to accommodate the operations used in PBEC.

(2) *Random 1D Clifford+T circuits (equivalence: original vs. optimized).* We generate random 1D Clifford+T circuits with the following gate-density profile (percent of gate placements): H 35%, S 35%, CNOT 10%, and T 20% (no identity gates), the same percentages used by Mei et al. [10]. Two-qubit gates are nearest-neighbor CNOTs on adjacent qubits, while single-qubit gates are sampled from $\{H, S, T\}$ according to the specified proportions. We evaluate circuits with $n \in \{32, 64, 128\}$ qubits.

For each configuration (n, depth) , we generate 100 random circuits (“original”) and apply PyZX optimization to obtain corresponding “optimized” circuits, resulting in 100 original/optimized pairs per (n, depth) . For the $n = 128$ setting, PyZX optimization becomes prohibitively slow at larger depths; consequently, in this case we directly optimize only circuits up to depth 7. To construct higher-depth instances at $n = 128$, we randomly sample circuit blocks of depth in $\{2, \dots, 7\}$, apply PyZX optimization at the block level, and then concatenate these optimized blocks until reaching the target depth, forming the corresponding high-depth original/optimized pairs. Consequently, the “optimized” circuits in the $n = 128$ experiments are best viewed as *semi-optimized* (or *pseudo-optimized*) rather than globally optimized for the full target depth. This approximation does not affect fairness: both equivalence checkers are evaluated on exactly the same circuit pairs generated by the identical procedure, and the same semi-optimization pipeline is applied uniformly across all methods.

We measure the runtime of equivalence checking on each pair with a per-instance timeout of 100 seconds. We report: (i) *completion rate*, the percentage of instances that terminate before timeout, and (ii) *success rate*, the percentage of *completed* instances that return the correct equivalence outcome.

(3) *Random Clifford+T circuits (inequivalence: optimized vs. mutated optimized).* To evaluate inequivalence detection under controlled perturbations, we compare the original circuit against a mutated version of the optimized circuit from (2) by removing one randomly chosen gate from the optimized circuit. We then check $\langle \text{original}, \text{mutated-optimized} \rangle$ pairs, which are inequivalent by construction. All other settings match (2): the same (n, depth) grid, 100 pairs per configuration, a 100-second timeout, and the same completion-rate and success-rate metrics.

(4) *Procedure for generating random Random Clifford+T circuits.* Random Clifford+T circuits are generated layer-by-layer. For each layer, qubits are scanned from left to right. At each qubit position q , we first attempt to place a nearest-neighbor two-qubit gate: with probability p_{CNOT} , we apply a CNOT on $(q, q+1)$ (if $q < n-1$) and then skip the next qubit position (i.e., advance by two). Otherwise, with probability p_I we place no gate on q and advance by one. If neither event occurs, we place a single-qubit gate on q , sampled from $\{H, S, T\}$ with relative weights proportional to (p_H, p_S, p_T) (normalized so the three weights sum to 1), and then advance by one. Repeating this procedure for the specified number of layers yields the circuit. In our experiments, we set $p_I = 0$ and use the gate-density profile $p_H = 0.35$, $p_S = 0.35$, $p_{\text{CNOT}} = 0.10$, and $p_T = 0.20$.

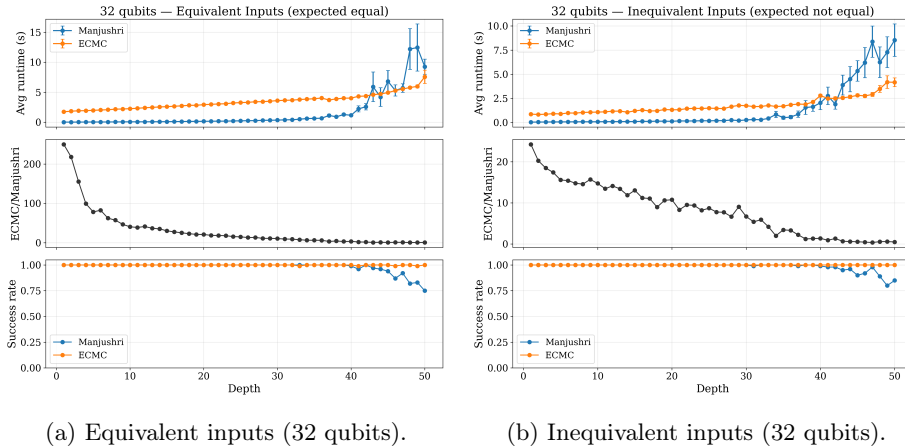


Fig. 1: Results for 32-qubit random-circuit benchmarks.

(5) *Algorithmic circuits with injected-error variants.* We additionally benchmark on the quantum-algorithm circuit suite distributed with the ECMC–QUOKKA-SHARP artifacts [10], which is the same benchmark set used in ECMC’s published comparison with QCEC [7]. For each original circuit, the artifact provides paired variants with known expected outcomes: *opt* (optimized circuit, expected equivalent), and four inequivalence injections—*gm* (gate-missing variant), *flip* (CNOT control/target flipped), *shift4* (phase-shift of magnitude 10^{-4}), and *shift7* (phase-shift of magnitude 10^{-7}).

3.2 Results and Findings

Figures 1 to 3 report the results of our experiments on circuit pairs with 32, 64, and 128 qubits, respectively. Each panel reports (top) the average runtime versus depth, with error bars showing the standard error of the mean (SEM); (middle) the runtime ratio (ECMC / MANJUSHRI); and (bottom) the success rate. Only runtimes for runs that do not time out and do produce correct results are counted in computing the means.

Table 1 shows aggregate statistics over all 5,000 runs per n_{qubits} and input type. We found that ECMC does not always return correct results (see columns 5 and 7 in the rows for ECMC). We contacted the authors of the ECMC tool for help in diagnosing the source of error(s) in ECMC. They suggested changing the floating-point-error tolerance, which helps checking inequivalent inputs because it enforces harder conditions for returning the answer “equivalent.” Unfortunately, this change does not correct all issues: equivalence checking of ECMC still makes mistakes. We will try to work with them after the submission deadline to identify and correct the root cause.

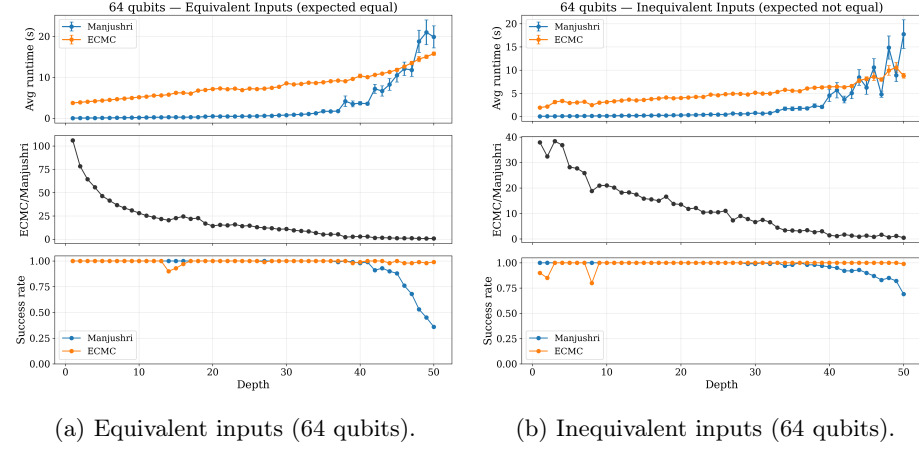


Fig. 2: Results for 64-qubit random-circuit benchmarks.

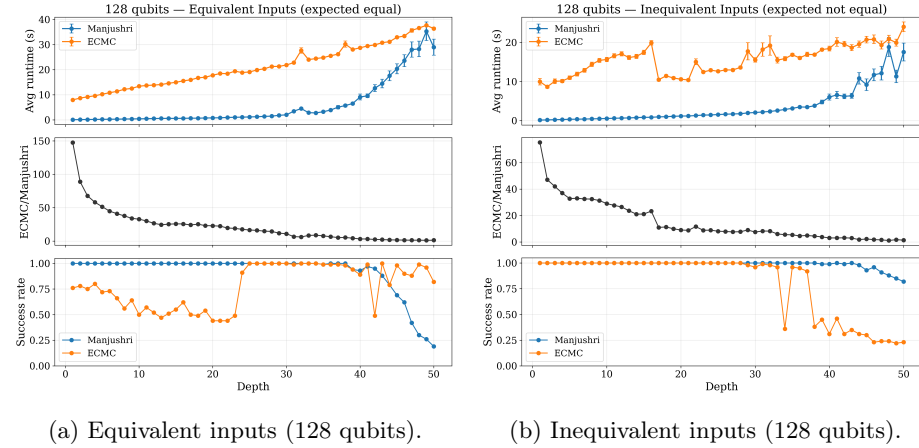


Fig. 3: Results for 128-qubit random-circuit benchmarks.

Findings. The experiments reveal that there is a trade-off between MANJUSHRI and ECMC. The fact that such a trade-off exists is not surprising, given that they are based on radically different techniques.

- For circuits of 32, 64, and 128 qubits, MANJUSHRI is faster for shallower circuits; ECMC is faster for deeper circuits. The circuit depths at the respective crossover points are as follows:

Table 1: Aggregate statistics over all 5,000 runs per n_{qubits} and input type, obtained from the 50 circuit depths $1 \leq d \leq 50$, with 100 independent circuit pairs (equivalent or inequivalent) at each depth. We report the completion rate, the correctness rate (percentage of correct results across runs that did not time out), the success rate (percentage of correct results across all the runs), and the number of incorrect (non-timeout) outcomes.

n_{qubits}	Input	Method	Completion	Correctness	Success (non-timeout)	Incorrect
32	equivalent	ECMC	99.98%	99.92%	99.90%	4
64	equivalent	ECMC	100.00%	99.32%	99.32%	34
128	equivalent	ECMC	98.02%	79.49%	77.92%	1005
32	inequivalent	ECMC	100.00%	100.00%	100.00%	0
64	inequivalent	ECMC	99.98%	99.10%	99.08%	45
128	inequivalent	ECMC	97.82%	81.89%	80.10%	886
32	equivalent	MANJUSHRI	98.32%	100.00%	98.32%	0
64	equivalent	MANJUSHRI	94.72%	100.00%	94.72%	0
128	equivalent	MANJUSHRI	91.86%	100.00%	91.86%	0
32	inequivalent	MANJUSHRI	98.36%	100.00%	98.36%	0
64	inequivalent	MANJUSHRI	96.98%	100.00%	96.98%	0
128	inequivalent	MANJUSHRI	98.60%	100.00%	98.60%	0

Qubits	Depth	
	Equivalent inputs	Inequivalent inputs
32	43	40
64	41	39
128	44	49

- Regardless of whether the result is “Equivalent” or “Inequivalent,” MANJUSHRI is much faster up to depth 30: when inputs are equivalent, MANJUSHRI is about 10 \times faster (or more); when inputs are inequivalent, MANJUSHRI is about 8 \times faster (or more).
- For both kinds of equivalence-checking outcomes, ECMC’s success rate out to depth 50 is impressive on 32- and 64-qubit circuits: on such circuits, ECMC is almost uniformly successful. However, ECMC struggled on 128-qubit circuits for some depths.

MANJUSHRI is almost uniformly successful out to about depth 38, before tailing off to about 75% at depth 50 (falling to 0% at depth 48 for 128-qubit circuits that are equivalent).

- For both tools, answers are obtained faster when the input circuits are inequivalent than when the input circuits are equivalent.

Algorithmic circuits with injected-error variants. The appendix gives the results of our experiment with the benchmark suite from the ECMC–QUOKKA–

SHARP artifacts¹⁰ (an ECMC benchmark used in multiple papers from that group).

4 Artifact Submission

If the paper is accepted, we intend to submit an artifact for evaluation.

5 Conclusion

Section 3 presents an extensive experimental evaluation that, for random 1D Clifford+ T circuits, explores the trade-off between MANJUSHRI and ECMC.

A natural application for both ECMC and MANJUSHRI would be for checking circuit fragments in a circuit optimizer [19], or circuit-optimizer generator [18]. Our colleague Amanda Xu told us that both (i) the circuit fragments analyzed to create rewrite rules, and (ii) the sub-circuits that are resynthesized in her tools have no more than 3–5 qubits, and that the rewrite-rule patterns are at most depth 6 [17]. Both ECMC and MANJUSHRI can check equivalence of much larger circuits than that, so it might be possible to use them in an optimizer that resynthesizes larger subcircuits (with more qubits) than can currently be handled using unitary synthesis (the standard technique). Because MANJUSHRI (a) is so much faster than ECMC on circuits out to depth 30 (with the crossover point varying from 39–49), and (b) is almost uniformly successful out to about depth 38, MANJUSHRI would be the preferred choice until optimizers are created that need to check equivalence of sub-circuits of depth > 38 .

¹⁰ <https://github.com/System-Verification-Lab/quokka-sharp-artifacts/tree/main/benchmark/algorithm>

References

1. Bahar, R., Frohm, E., Gaona, C., Hachtel, G., Macii, E., Pardo, A., Somenzi, F.: Algebraic decision diagrams and their applications. In: International Conference on Computer Aided Design (ICCAD) (1993)
2. Barthe, G., Grégoire, B., Zanella Béguelin, S.: Formal certification of code-based cryptographic proofs. In: Proceedings of the 36th Annual ACM SIGPLAN-SIGACT Symposium on Principles of Programming Languages. pp. 90–101. POPL ’09, Association for Computing Machinery, New York, NY, USA (2009). <https://doi.org/10.1145/1480881.1480894>, <https://doi.org.ezproxy.lib.uts.edu.au/10.1145/1480881.1480894>
3. Barthe, G., Hsu, J., Ying, M., Yu, N., Zhou, L.: Relational proofs for quantum programs. Proc. ACM Program. Lang. 4(POPL) (Dec 2019). <https://doi.org/10.1145/3371089>, <https://doi.org/10.1145/3371089>
4. Barthe, G., Köpf, B., Olmedo, F., Zanella-Béguelin, S.: Probabilistic relational reasoning for differential privacy. ACM Trans. Program. Lang. Syst. 35(3) (Nov 2013). <https://doi.org/10.1145/2492061>, <https://doi.org/10.1145/2492061>
5. Benton, N.: Simple relational correctness proofs for static analyses and program transformations. In: Proceedings of the 31st ACM SIGPLAN-SIGACT Symposium on Principles of Programming Languages. pp. 14–25. POPL ’04, Association for Computing Machinery, New York, NY, USA (2004). <https://doi.org/10.1145/964001.964003>, <https://doi.org.ezproxy.lib.uts.edu.au/10.1145/964001.964003>
6. Bergstra, J., Tiuryn, J., Tucker, J.: Floyd’s principle, correctness theories and program equivalence. Theoretical Computer Science 17(2), 113–149 (1982). [https://doi.org/https://doi.org/10.1016/0304-3975\(82\)90001-9](https://doi.org/https://doi.org/10.1016/0304-3975(82)90001-9), <https://www.sciencedirect.com/science/article/pii/0304397582900019>
7. Burgholzer, L., Wille, R.: Advanced equivalence checking for quantum circuits. IEEE Transactions on Computer-Aided Design of Integrated Circuits and Systems 40(9), 1810–1824 (2020)
8. Kissinger, A., Van De Wetering, J.: PyZX: Large scale automated diagrammatic reasoning. QPL pp. 229–241 (2019)
9. Li, Y., Unruh, D.: Quantum Relational Hoare Logic with Expectations. In: Bansal, N., Merelli, E., Worrell, J. (eds.) 48th International Colloquium on Automata, Languages, and Programming (ICALP 2021). Leibniz International Proceedings in Informatics (LIPIcs), vol. 198, pp. 136:1–136:20. Schloss Dagstuhl – Leibniz-Zentrum für Informatik, Dagstuhl, Germany (2021). <https://doi.org/10.4230/LIPIcs.ICALP.2021.136>, <https://drops.dagstuhl.de/opus/volltexte/2021/14205>
10. Mei, J., Coopmans, T., Bonsangue, M.M., Laarman, A.: Equivalence checking of quantum circuits by model counting. In: Automated Reasoning, Lecture Notes in Computer Science, vol. 14740, pp. 401–421. Springer, Cham (2024)
11. Necula, G.C.: Translation validation for an optimizing compiler. SIGPLAN Not. 35(5), 83–94 (May 2000). <https://doi.org/10.1145/358438.349314>, <https://doi.org/10.1145/358438.349314>
12. Rand, R., Paykin, J., Zdancewic, S.: QWIRE practice: Formal verification of quantum circuits in coq. Electronic Proceedings in Theoretical Computer Science 266, 119–132 (Feb 2018). <https://doi.org/10.4204/eptcs.266.8>, <http://dx.doi.org/10.4204/EPTCS.266.8>
13. Sistla, M., Chaudhuri, S., Reps, T.: Symbolic quantum simulation with Quasimodo. In: International Conference on Computer Aided Verification. pp. 213–225. Springer (2023)

14. Sistla, M., Chaudhuri, S., Reps, T.: Weighted context-free-language ordered binary decision diagrams. *Proceedings of the ACM on Programming Languages* **8**(OOPSLA2), 1390–1419 (2024)
15. Sistla, M.A., Chaudhuri, S., Reps, T.: Cflobdds: Context-free-language ordered binary decision diagrams. *ACM Transactions on Programming Languages and Systems* **46**(2), 1–82 (2024)
16. Unruh, D.: Quantum relational hoare logic. *Proc. ACM Program. Lang.* **3**(POPL) (Jan 2019). <https://doi.org/10.1145/3290346>, <https://doi.org/10.1145/3290346>
17. Xu, A.: (Jan 2026), personal communication
18. Xu, A., Molavi, A., Pick, L., Tannu, S., Albarghouthi, A.: Synthesizing quantum-circuit optimizers. In: *ACM SIGPLAN Conference on Programming Language Design and Implementation (PLDI)* (2023)
19. Xu, A., Molavi, A., Tannu, S., Albarghouthi, A.: Optimizing quantum circuits, fast and slow. In: *International Conference on Architectural Support for Programming Languages and Operating Systems (ASPLOS)* (2025)
20. Yan, P., Jiang, H., Yu, N.: On incorrectness logic for quantum programs. *Proc. ACM Program. Lang.* **6**(OOPSLA1) (Apr 2022). <https://doi.org/10.1145/3527316>, <https://doi.org/10.1145/3527316>
21. Yan, P., Jiang, H., Yu, N.: Approximate relational reasoning for quantum programs. In: *Computer Aided Verification, Lecture Notes in Computer Science*, vol. 14683, pp. 495–519. Springer (2024)
22. Ying, M.: Foundations of Quantum Programming. Morgan Kaufmann Publishers Inc., San Francisco, CA, USA, 1st edn. (2016). <https://doi.org/10.1016/C2014-0-02660-3>
23. Ying, M., Duan, R., Feng, Y., Ji, Z.: Predicate Transformer Semantics of Quantum Programs, pp. 311–360. Cambridge University Press, Cambridge (2009). <https://doi.org/10.1017/CBO9781139193313.009>
24. Yu, N., Trinh, X.D., Reps, T.: Scalable equivalence checking and verification of shallow quantum circuits. *Proc. ACM Program. Lang.* **9**(OOPSLA2) (Oct 2025). <https://doi.org/10.1145/3763153>, <https://doi.org/10.1145/3763153>
25. Zulehner, A., Hillmich, S., Wille, R.: How to efficiently handle complex values? implementing decision diagrams for quantum computing. In: *2019 IEEE/ACM International Conference on Computer-Aided Design (ICCAD)*. pp. 1–7. IEEE (2019)

Appendix

This section give the results of our experiment with the benchmark suite from the ECMC–QUOKKA–SHARP artifacts [10], which is the benchmark set used in ECMC’s published comparison with QCEC [7]. For each original circuit, the artifact provides paired variants with known expected outcomes: *opt* (optimized circuit, expected equivalent), and four inequivalence injections—*gm* (gate-missing variant), *flip* (CNOT control/target flipped), *shift4* (phase-shift of magnitude 10^{-4}), and *shift7* (phase-shift of magnitude 10^{-7}).

When both ECMC and MANJUSHRI timed out on a circuit, we do not list it in the tables in this appendix.

Table 2: *cycle10_293*: cases where at least one method completed (incorrect results shown in bold).

Circuit	<i>n</i>	$ G $	$ G' $	variant	ECMC	MANJUSHRI
<i>cycle10_293</i>	39	512	846	gm	1.12	TO
<i>cycle10_293</i>	39	512	847	opt	TO	21.42

Table 3: *dj*: cases where at least one method completed (incorrect results shown in bold). For 16-, 32-, and 64-qubit shift4, the expected answer is “Inequivalent.” Both ECMC and MANJUSHRI reported “Equivalent,” which is actually the correct answer because those circuits contain no occurrences of R_z , and thus no opportunity to inject a rotation error.

Circuit	<i>n</i>	$ G $	$ G' $	variant	ECMC	MANJUSHRI
<i>dj_nativegates_ibm_qiskit</i>	16	127	67	flip	0.67	0.07
<i>dj_nativegates_ibm_qiskit</i>	16	127	66	gm	0.39	0.05
<i>dj_nativegates_ibm_qiskit</i>	16	127	67	opt	2.01	0.13
<i>dj_nativegates_ibm_qiskit</i>	16	127	67	shift4	[0.80]	[0.13]
<i>dj_nativegates_ibm_qiskit</i>	16	127	67	shift7	0.78	0.09
<i>dj_nativegates_ibm_qiskit</i>	32	249	129	flip	0.91	TO
<i>dj_nativegates_ibm_qiskit</i>	32	249	128	gm	0.72	TO
<i>dj_nativegates_ibm_qiskit</i>	32	249	129	opt	2.13	0.56
<i>dj_nativegates_ibm_qiskit</i>	32	249	129	shift4	[1.79]	[0.54]
<i>dj_nativegates_ibm_qiskit</i>	32	249	129	shift7	1.64	TO
<i>dj_nativegates_ibm_qiskit</i>	64	507	259	flip	1.40	TO
<i>dj_nativegates_ibm_qiskit</i>	64	507	258	gm	1.26	TO
<i>dj_nativegates_ibm_qiskit</i>	64	507	259	opt	4.68	3.14
<i>dj_nativegates_ibm_qiskit</i>	64	507	259	shift4	[3.94]	[2.97]
<i>dj_nativegates_ibm_qiskit</i>	64	507	259	shift7	6.91	TO

Table 4: **ghz**: cases where at least one method completed (incorrect results shown in bold).

Circuit	<i>n</i>	<i>G</i>	<i>G'</i>	variant	ECMC	MANJUSHRI
ghz_nativegates_ibm_qiskit	16	18	45	gm	0.38	0.06
ghz_nativegates_ibm_qiskit	16	18	46	opt	0.88	0.09
ghz_nativegates_ibm_qiskit	32	34	93	gm	0.93	TO
ghz_nativegates_ibm_qiskit	32	34	94	opt	1.82	0.39
ghz_nativegates_ibm_qiskit	64	66	189	gm	1.84	TO
ghz_nativegates_ibm_qiskit	64	66	190	opt	3.82	1.75

Table 5: **graphstate**: cases where at least one method completed (incorrect results shown in bold).

Circuit	<i>n</i>	<i>G</i>	<i>G'</i>	variant	ECMC	MANJUSHRI
graphstate_nativegates_ibm_qiskit	16	160	31	gm	0.80	0.06
graphstate_nativegates_ibm_qiskit	16	160	32	opt	1.04	0.15
graphstate_nativegates_ibm_qiskit	32	320	63	gm	1.29	0.09
graphstate_nativegates_ibm_qiskit	32	320	64	opt	1.97	0.18
graphstate_nativegates_ibm_qiskit	64	640	127	gm	3.68	0.20
graphstate_nativegates_ibm_qiskit	64	640	128	opt	8.34	0.43

Table 6: **groundstate_medium**: cases where at least one method completed (incorrect results shown in bold).

Circuit	<i>n</i>	<i>G</i>	<i>G'</i>	variant	ECMC	MANJUSHRI
groundstate_medium_nativegates_qiskit	12	1212	164	flip	TO	1.55
groundstate_medium_nativegates_qiskit	12	1212	163	gm	TO	1.57
groundstate_medium_nativegates_qiskit	12	1212	164	shift4	TO	1.28
groundstate_medium_nativegates_qiskit	12	1212	164	shift7	TO	1.71

Table 7: **groundstate_small**: cases where at least one method completed (incorrect results shown in bold).

Circuit	<i>n</i>	<i>G</i>	<i>G'</i>	variant	ECMC	MANJUSHRI
groundstate_small_nativegates_qiskit	4	180	35	gm	0.14	0.05
groundstate_small_nativegates_qiskit	4	180	36	opt	0.39	0.09
groundstate_small_nativegates_qiskit	4	180	36	shift4	0.15	0.06
groundstate_small_nativegates_qiskit	4	180	36	shift7	0.43	0.04

Table 8: **grover-noancilla**: cases where at least one method completed (incorrect results shown in bold).

Circuit	<i>n</i>	<i>G</i>	<i>G'</i>	variant	ECMC	MANJUSHRI
grover-noancilla_nativegates_ibm_qiskit 3	190	190	flip	0.36	0.26	
grover-noancilla_nativegates_ibm_qiskit 3	190	189	gm	0.35	0.16	
grover-noancilla_nativegates_ibm_qiskit 3	190	190	opt	1.05	0.30	
grover-noancilla_nativegates_ibm_qiskit 3	190	190	shift4	0.44	15.36	
grover-noancilla_nativegates_ibm_qiskit 3	190	190	shift7	1.19	4.56	
grover-noancilla_nativegates_ibm_qiskit 4	499	629	flip	8.85	27.14	
grover-noancilla_nativegates_ibm_qiskit 4	499	628	gm	10.61	3.83	
grover-noancilla_nativegates_ibm_qiskit 4	499	629	opt	43.24	TO	
grover-noancilla_nativegates_ibm_qiskit 4	499	629	shift4	10.36	TO	
grover-noancilla_nativegates_ibm_qiskit 4	499	629	shift7	13.29	TO	

Table 9: *grover-v-chain*: cases where at least one method completed (incorrect results shown in bold).

Circuit	n	$ G $	$ G' $	variant	ECMC	MANJUSHRI
grover-v-chain_nativegates_ibm_qiskit	4	529	632	flip	29.98	24.58
grover-v-chain_nativegates_ibm_qiskit	4	529	631	gm	30.07	7.51
grover-v-chain_nativegates_ibm_qiskit	4	529	632	shift4	26.58	TO

Table 10: *portfolioqaoa*: cases where at least one method completed (incorrect results shown in bold).

Circuit	n	$ G $	$ G' $	variant	ECMC	MANJUSHRI
portfolioqaoa_nativegates_ibm_qiskit	5	195	236	flip	7.33	32.65
portfolioqaoa_nativegates_ibm_qiskit	5	195	235	gm	6.94	16.47
portfolioqaoa_nativegates_ibm_qiskit	5	195	236	opt	9.60	TO
portfolioqaoa_nativegates_ibm_qiskit	5	195	236	shift4	5.67	11.22
portfolioqaoa_nativegates_ibm_qiskit	5	195	236	shift7	12.30	18.72
portfolioqaoa_nativegates_ibm_qiskit	6	261	356	flip	79.16	TO
portfolioqaoa_nativegates_ibm_qiskit	6	261	355	gm	73.19	TO
portfolioqaoa_nativegates_ibm_qiskit	6	261	356	shift4	15.10	TO

Table 11: *portfolioqvqe*: cases where at least one method completed (incorrect results shown in bold).

Circuit	n	$ G $	$ G' $	variant	ECMC	MANJUSHRI
portfolioqvqe_nativegates_ibm_qiskit	5	310	131	flip	6.64	4.68
portfolioqvqe_nativegates_ibm_qiskit	5	310	130	gm	5.51	5.63
portfolioqvqe_nativegates_ibm_qiskit	5	310	131	opt	8.27	TO
portfolioqvqe_nativegates_ibm_qiskit	5	310	131	shift4	6.58	TO
portfolioqvqe_nativegates_ibm_qiskit	5	310	131	shift7	8.17	84.18
portfolioqvqe_nativegates_ibm_qiskit	6	435	151	flip	41.77	34.62
portfolioqvqe_nativegates_ibm_qiskit	6	435	150	gm	35.18	52.99
portfolioqvqe_nativegates_ibm_qiskit	6	435	151	shift4	46.68	TO

Table 12: *pricingcall*: cases where at least one method completed (incorrect results shown in bold).

Circuit	n	$ G $	$ G' $	variant	ECMC	MANJUSHRI
pricingcall_nativegates_ibm_qiskit	5	240	166	flip	0.51	0.20
pricingcall_nativegates_ibm_qiskit	5	240	165	gm	0.42	0.22
pricingcall_nativegates_ibm_qiskit	5	240	166	opt	4.29	0.44
pricingcall_nativegates_ibm_qiskit	5	240	166	shift4	0.47	54.65
pricingcall_nativegates_ibm_qiskit	5	240	166	shift7	2.45	TO
pricingcall_nativegates_ibm_qiskit	7	422	277	flip	7.95	1.32
pricingcall_nativegates_ibm_qiskit	7	422	276	gm	6.33	0.62
pricingcall_nativegates_ibm_qiskit	7	422	277	opt	15.03	50.81
pricingcall_nativegates_ibm_qiskit	7	422	277	shift4	5.94	TO
pricingcall_nativegates_ibm_qiskit	7	422	277	shift7	83.05	TO

Table 13: **pricingput**: cases where at least one method completed (incorrect results shown in bold).

Circuit	n	$ G $	$ G' $	variant	ECMC	MANJUSHRI
pricingput_nativegates_ibm_qiskit	5	240	192	flip	0.28	0.12
pricingput_nativegates_ibm_qiskit	5	240	191	gm	0.24	0.13
pricingput_nativegates_ibm_qiskit	5	240	192	opt	2.25	0.46
pricingput_nativegates_ibm_qiskit	5	240	192	shift4	1.34	0.43
pricingput_nativegates_ibm_qiskit	5	240	192	shift7	2.41	7.22
pricingput_nativegates_ibm_qiskit	7	432	297	flip	19.65	1.74
pricingput_nativegates_ibm_qiskit	7	432	296	gm	8.31	0.66
pricingput_nativegates_ibm_qiskit	7	432	297	opt	TO	10.35
pricingput_nativegates_ibm_qiskit	7	432	297	shift4	8.64	TO
pricingput_nativegates_ibm_qiskit	9	654	428	opt	19.78	TO

Table 14: **qaoa**: cases where at least one method completed (incorrect results shown in bold).

Circuit	n	$ G $	$ G' $	variant	ECMC	MANJUSHRI
qaoa_nativegates_ibm_qiskit	7	133	117	flip	0.33	0.17
qaoa_nativegates_ibm_qiskit	7	133	116	gm	0.18	0.06
qaoa_nativegates_ibm_qiskit	7	133	117	opt	0.58	0.23
qaoa_nativegates_ibm_qiskit	7	133	117	shift4	0.16	0.15
qaoa_nativegates_ibm_qiskit	7	133	117	shift7	0.55	0.15
qaoa_nativegates_ibm_qiskit	9	171	296	flip	0.35	0.22
qaoa_nativegates_ibm_qiskit	9	171	295	gm	0.36	TO
qaoa_nativegates_ibm_qiskit	9	171	296	opt	0.97	2.30
qaoa_nativegates_ibm_qiskit	9	171	296	shift4	0.40	2.73
qaoa_nativegates_ibm_qiskit	9	171	296	shift7	1.08	TO
qaoa_nativegates_ibm_qiskit	11	209	359	flip	0.71	1.54
qaoa_nativegates_ibm_qiskit	11	209	358	gm	0.36	0.55
qaoa_nativegates_ibm_qiskit	11	209	359	opt	1.01	2.28
qaoa_nativegates_ibm_qiskit	11	209	359	shift4	0.31	0.65
qaoa_nativegates_ibm_qiskit	11	209	359	shift7	1.27	0.33
qaoa_nativegates_ibm_qiskit	14	266	280	flip	0.44	0.08
qaoa_nativegates_ibm_qiskit	14	266	279	gm	0.42	0.53
qaoa_nativegates_ibm_qiskit	14	266	280	opt	1.20	0.97
qaoa_nativegates_ibm_qiskit	14	266	280	shift4	0.42	0.50
qaoa_nativegates_ibm_qiskit	14	266	280	shift7	1.29	0.33
qaoa_nativegates_ibm_qiskit	15	285	587	flip	0.48	0.87
qaoa_nativegates_ibm_qiskit	15	285	586	gm	0.59	3.11
qaoa_nativegates_ibm_qiskit	15	285	587	opt	2.59	5.61
qaoa_nativegates_ibm_qiskit	15	285	587	shift4	0.62	0.44
qaoa_nativegates_ibm_qiskit	15	285	587	shift7	2.71	0.56
qaoa_nativegates_ibm_qiskit	16	304	461	flip	0.56	TO
qaoa_nativegates_ibm_qiskit	16	304	460	gm	0.45	0.98
qaoa_nativegates_ibm_qiskit	16	304	461	opt	1.42	4.38
qaoa_nativegates_ibm_qiskit	16	304	461	shift4	0.91	69.36
qaoa_nativegates_ibm_qiskit	16	304	461	shift7	1.58	2.00

Table 15: `qft`: cases where at least one method completed (incorrect results shown in bold).

Circuit	n	$ G $	$ G' $	variant	ECMC	MANJUSHRI
<code>qft_nativegates_ibm_qiskit</code>	2	14	14	flip	0.11	0.03
<code>qft_nativegates_ibm_qiskit</code>	2	14	13	gm	0.10	0.02
<code>qft_nativegates_ibm_qiskit</code>	2	14	14	opt	0.10	0.03
<code>qft_nativegates_ibm_qiskit</code>	2	14	14	shift4	0.10	0.03
<code>qft_nativegates_ibm_qiskit</code>	2	14	14	shift7	0.10	0.03
<code>qft_nativegates_ibm_qiskit</code>	8	176	228	flip	0.24	0.27
<code>qft_nativegates_ibm_qiskit</code>	8	176	227	gm	0.24	0.17
<code>qft_nativegates_ibm_qiskit</code>	8	176	228	opt	3.40	1.88
<code>qft_nativegates_ibm_qiskit</code>	8	176	228	shift4	0.30	TO
<code>qft_nativegates_ibm_qiskit</code>	8	176	228	shift7	1.38	TO
<code>qft_nativegates_ibm_qiskit</code>	16	672	814	flip	1.50	TO
<code>qft_nativegates_ibm_qiskit</code>	16	672	813	gm	0.83	TO
<code>qft_nativegates_ibm_qiskit</code>	16	672	814	opt	1.73	TO
<code>qft_nativegates_ibm_qiskit</code>	16	672	814	shift4	1.15	TO
<code>qft_nativegates_ibm_qiskit</code>	32	2624	3176	gm	73.01	TO
<code>qft_nativegates_ibm_qiskit</code>	32	2624	3177	opt	70.83	TO
<code>qft_nativegates_ibm_qiskit</code>	32	2624	3177	shift4	72.25	TO
<code>qft_nativegates_ibm_qiskit</code>	32	2624	3177	shift7	71.32	TO

Table 16: `qftentangled`: cases where at least one method completed (incorrect results shown in bold).

Circuit	n	$ G $	$ G' $	variant	ECMC	MANJUSHRI
<code>qftentangled_nativegates_ibm_qiskit</code>	16	690	853	flip	0.61	TO
<code>qftentangled_nativegates_ibm_qiskit</code>	16	690	852	gm	51.73	TO
<code>qftentangled_nativegates_ibm_qiskit</code>	16	690	853	opt	51.60	TO
<code>qftentangled_nativegates_ibm_qiskit</code>	16	690	853	shift4	0.82	TO

Table 17: `qnn`: cases where at least one method completed (incorrect results shown in bold).

Circuit	n	$ G $	$ G' $	variant	ECMC	MANJUSHRI
<code>qnn_nativegates_ibm_qiskit</code>	2	43	36	flip	0.11	0.03
<code>qnn_nativegates_ibm_qiskit</code>	2	43	35	gm	0.10	0.03
<code>qnn_nativegates_ibm_qiskit</code>	2	43	36	opt	0.13	0.03
<code>qnn_nativegates_ibm_qiskit</code>	2	43	36	shift4	0.10	0.04
<code>qnn_nativegates_ibm_qiskit</code>	2	43	36	shift7	0.14	0.03
<code>qnn_nativegates_ibm_qiskit</code>	8	319	494	flip	0.40	TO
<code>qnn_nativegates_ibm_qiskit</code>	32	3583	8216	shift4	8.39	TO
<code>qnn_nativegates_ibm_qiskit</code>	32	3583	8216	shift7	7.31	TO

Table 18: `qpeexact`: cases where at least one method completed (incorrect results shown in bold).

Circuit	n	$ G $	$ G' $	variant	ECMC	MANJUSHRI
<code>qpeexact_nativegates_ibm_qiskit</code>	15	712	837	flip	1.05	TO
<code>qpeexact_nativegates_ibm_qiskit</code>	15	712	836	gm	1.31	TO
<code>qpeexact_nativegates_ibm_qiskit</code>	15	712	837	opt	68.48	TO
<code>qpeexact_nativegates_ibm_qiskit</code>	15	712	837	shift4	0.88	TO
<code>qpeexact_nativegates_ibm_qiskit</code>	31	2712	3276	flip	7.18	TO
<code>qpeexact_nativegates_ibm_qiskit</code>	31	2712	3276	shift4	7.94	TO

Table 19: **qpeinexact**: cases where at least one method completed (incorrect results shown in bold).

Circuit	<i>n</i>	<i>G</i>	<i>G'</i>	variant	ECMC	MANJUSHRI
qpeinexact_nativegates_ibm_qiskit	15	712	848	flip	3.21	TO
qpeinexact_nativegates_ibm_qiskit	15	712	847	gm	4.50	TO
qpeinexact_nativegates_ibm_qiskit	15	712	848	opt	11.07	TO
qpeinexact_nativegates_ibm_qiskit	15	712	848	shift4	0.72	TO
qpeinexact_nativegates_ibm_qiskit	31	2712	3179	flip	6.27	TO

Table 20: **rd84_313**: cases where at least one method completed (incorrect results shown in bold).

Circuit	<i>n</i>	<i>G</i>	<i>G'</i>	variant	ECMC	MANJUSHRI
rd84_313	34	804	1233	flip	1.32	TO
rd84_313	34	804	1292	gm	TO	55.93

Table 21: **realmprandom**: cases where at least one method completed (incorrect results shown in bold).

Circuit	<i>n</i>	<i>G</i>	<i>G'</i>	variant	ECMC	MANJUSHRI
realmprandom_nativegates_ibm_qiskit	16	680	678	gm	1.15	TO
realmprandom_nativegates_ibm_qiskit	16	680	679	opt	2.26	TO
realmprandom_nativegates_ibm_qiskit	32	2128	2215	flip	4.93	TO
realmprandom_nativegates_ibm_qiskit	32	2128	2215	opt	25.43	TO
realmprandom_nativegates_ibm_qiskit	32	2128	2215	shift4	25.89	TO
realmprandom_nativegates_ibm_qiskit	64	7328	7410	gm	21.54	TO
realmprandom_nativegates_ibm_qiskit	64	7328	7411	opt	28.10	TO

Table 22: **routing**: cases where at least one method completed (incorrect results shown in bold).

Circuit	<i>n</i>	<i>G</i>	<i>G'</i>	variant	ECMC	MANJUSHRI
routing_nativegates_ibm_qiskit	2	43	29	flip	0.10	0.03
routing_nativegates_ibm_qiskit	2	43	28	gm	0.11	0.03
routing_nativegates_ibm_qiskit	2	43	29	opt	0.14	0.04
routing_nativegates_ibm_qiskit	2	43	29	shift4	0.10	0.03
routing_nativegates_ibm_qiskit	2	43	29	shift7	0.13	0.03
routing_nativegates_ibm_qiskit	6	135	142	flip	0.40	0.23
routing_nativegates_ibm_qiskit	6	135	141	gm	0.39	70.65
routing_nativegates_ibm_qiskit	6	135	142	opt	20.91	TO
routing_nativegates_ibm_qiskit	6	135	142	shift4	0.34	TO
routing_nativegates_ibm_qiskit	6	135	142	shift7	5.77	TO
routing_nativegates_ibm_qiskit	12	273	409	flip	0.45	TO
routing_nativegates_ibm_qiskit	12	273	409	opt	4.43	TO
routing_nativegates_ibm_qiskit	12	273	409	shift4	6.48	TO
routing_nativegates_ibm_qiskit	12	273	409	shift7	18.02	TO

Table 23: **su2random**: cases where at least one method completed (incorrect results shown in bold).

Circuit	<i>n</i>	<i>G</i>	<i>G'</i>	variant	ECMC	MANJUSHRI
su2random_nativegates_ibm_qiskit	4	114	89	gm	0.14	0.07
su2random_nativegates_ibm_qiskit	4	114	90	opt	0.86	0.48
su2random_nativegates_ibm_qiskit	4	114	90	shift4	0.13	0.32
su2random_nativegates_ibm_qiskit	4	114	90	shift7	0.63	0.16
su2random_nativegates_ibm_qiskit	8	276	185	gm	1.67	6.14
su2random_nativegates_ibm_qiskit	8	276	186	shift4	41.97	TO
su2random_nativegates_ibm_qiskit	16	744	377	gm	3.34	TO
su2random_nativegates_ibm_qiskit	16	744	378	opt	10.27	TO
su2random_nativegates_ibm_qiskit	17	816	401	gm	2.60	TO
su2random_nativegates_ibm_qiskit	17	816	402	opt	2.69	TO
su2random_nativegates_ibm_qiskit	17	816	402	shift4	10.52	TO
su2random_nativegates_ibm_qiskit	19	969	450	shift4	1.09	TO
su2random_nativegates_ibm_qiskit	19	969	450	shift7	35.51	TO
su2random_nativegates_ibm_qiskit	32	2256	762	shift4	21.41	TO
su2random_nativegates_ibm_qiskit	32	2256	762	shift7	4.87	TO

Table 24: **tsp**: cases where at least one method completed (incorrect results shown in bold).

Circuit	<i>n</i>	<i>G</i>	<i>G'</i>	variant	ECMC	MANJUSHRI
tsp_nativegates_ibm_qiskit	4	225	86	flip	0.64	0.08
tsp_nativegates_ibm_qiskit	4	225	85	gm	0.71	0.09
tsp_nativegates_ibm_qiskit	4	225	86	opt	2.14	0.52
tsp_nativegates_ibm_qiskit	4	225	86	shift4	0.57	0.13
tsp_nativegates_ibm_qiskit	4	225	86	shift7	2.05	0.13
tsp_nativegates_ibm_qiskit	9	550	315	flip	TO	0.40
tsp_nativegates_ibm_qiskit	9	550	314	gm	TO	0.64
tsp_nativegates_ibm_qiskit	16	1005	623	flip	0.64	TO
tsp_nativegates_ibm_qiskit	16	1005	622	gm	37.15	TO

Table 25: **twolocalrandom**: cases where at least one method completed (incorrect results shown in bold).

Circuit	<i>n</i>	<i>G</i>	<i>G'</i>	variant	ECMC	MANJUSHRI
twolocalrandom_nativegates_ibm_qiskit	16	680	679	flip	56.93	TO
twolocalrandom_nativegates_ibm_qiskit	16	680	678	gm	0.99	TO
twolocalrandom_nativegates_ibm_qiskit	32	2128	2215	flip	4.97	TO
twolocalrandom_nativegates_ibm_qiskit	32	2128	2214	gm	5.00	TO
twolocalrandom_nativegates_ibm_qiskit	32	2128	2215	opt	24.31	TO
twolocalrandom_nativegates_ibm_qiskit	64	7328	7411	opt	32.27	TO

Table 26: `vqe`: cases where at least one method completed (incorrect results shown in bold).

Circuit	n	$ G $	$ G' $	variant	ECMC	MANJUSHRI
vqe_nativegates_ibm_qiskit	5	83	83	flip	0.14	0.03
vqe_nativegates_ibm_qiskit	5	83	82	gm	0.13	0.04
vqe_nativegates_ibm_qiskit	5	83	83	opt	0.48	83.52
vqe_nativegates_ibm_qiskit	5	83	83	shift4	0.15	0.87
vqe_nativegates_ibm_qiskit	5	83	83	shift7	0.36	0.40
vqe_nativegates_ibm_qiskit	10	168	221	flip	0.28	0.06
vqe_nativegates_ibm_qiskit	10	168	220	gm	0.79	TO
vqe_nativegates_ibm_qiskit	10	168	221	opt	1.70	TO
vqe_nativegates_ibm_qiskit	10	168	221	shift4	0.87	TO
vqe_nativegates_ibm_qiskit	10	168	221	shift7	1.52	TO
vqe_nativegates_ibm_qiskit	14	236	327	flip	0.45	0.23
vqe_nativegates_ibm_qiskit	14	236	326	gm	0.44	0.89
vqe_nativegates_ibm_qiskit	14	236	327	opt	1.93	TO
vqe_nativegates_ibm_qiskit	14	236	327	shift4	0.47	TO
vqe_nativegates_ibm_qiskit	14	236	327	shift7	4.56	1.61
vqe_nativegates_ibm_qiskit	15	253	349	flip	0.47	0.16
vqe_nativegates_ibm_qiskit	15	253	348	gm	0.46	0.54
vqe_nativegates_ibm_qiskit	15	253	349	opt	9.19	TO
vqe_nativegates_ibm_qiskit	15	253	349	shift4	0.63	TO
vqe_nativegates_ibm_qiskit	15	253	349	shift7	5.23	TO
vqe_nativegates_ibm_qiskit	16	270	424	flip	1.69	TO
vqe_nativegates_ibm_qiskit	16	270	423	gm	0.51	4.28
vqe_nativegates_ibm_qiskit	16	270	424	opt	7.03	TO
vqe_nativegates_ibm_qiskit	16	270	424	shift4	2.45	TO
vqe_nativegates_ibm_qiskit	16	270	424	shift7	8.75	TO

Table 27: `wstate`: cases where at least one method completed (incorrect results shown in bold).

Circuit	n	$ G $	$ G' $	variant	ECMC	MANJUSHRI
wstate_nativegates_ibm_qiskit	16	271	242	flip	0.73	0.17
wstate_nativegates_ibm_qiskit	16	271	241	gm	0.98	0.29
wstate_nativegates_ibm_qiskit	16	271	242	opt	1.65	0.44
wstate_nativegates_ibm_qiskit	16	271	242	shift4	0.59	0.15
wstate_nativegates_ibm_qiskit	16	271	242	shift7	1.48	0.10
wstate_nativegates_ibm_qiskit	32	559	498	flip	1.32	TO
wstate_nativegates_ibm_qiskit	32	559	497	gm	2.72	TO
wstate_nativegates_ibm_qiskit	32	559	498	opt	4.90	3.70
wstate_nativegates_ibm_qiskit	32	559	498	shift4	1.97	TO
wstate_nativegates_ibm_qiskit	32	559	498	shift7	5.24	TO
wstate_nativegates_ibm_qiskit	64	1135	1010	flip	4.77	TO
wstate_nativegates_ibm_qiskit	64	1135	1009	gm	9.21	TO
wstate_nativegates_ibm_qiskit	64	1135	1010	opt	19.49	39.38
wstate_nativegates_ibm_qiskit	64	1135	1010	shift4	4.46	TO
wstate_nativegates_ibm_qiskit	64	1135	1010	shift7	4.79	TO